FT-IR Spectroscopic Characterization of NADH:Ubiquinone Oxidoreductase (Complex I) from *Escherichia coli*: Oxidation of FeS Cluster N2 is Coupled with the Protonation of an Aspartate or Glutamate Side Chain†

Petra Hellwig,‡,§ Dierk Scheide,|| Stefanie Bungert,|| Werner Mäntele,‡ and Thorsten Friedrich*,||

Institut für Biophysik, Johann-Wolfgang-Goethe-Universität Theodor-Stern-Kai 7, Haus 74, 60590 Frankfurt/M., Germany, and Institut für Biochemie, Heinrich-Heine-Universität Universitätsstrasse 1, 40225 Düsseldorf, Germany

Received April 13, 2000; Revised Manuscript Received June 29, 2000

ABSTRACT: The proton-pumping NADH:ubiquinone oxidoreductase, also called complex I, is the first energy-transducing complex of many respiratory chains. It couples the transfer of electrons from NADH to ubiquinone with the translocation of protons across the membrane. One FMN and up to nine iron−sulfur (FeS) clusters participate in the redox reaction. So far, complex I has been described mainly by means of EPR- and UV−vis spectroscopy. Here, we report for the first time an infrared spectroscopic characterization of complex I. Electrochemically induced FT-IR difference spectra of complex I from *Escherichia coli* and of the NADH dehydrogenase fragment of this complex were obtained for critical potential steps. The spectral contributions of the FMN in both preparations were derived from a comparison using model compounds and turned out to be unexpectedly small. Furthermore, the FT-IR difference spectra reveal that the redox transitions of the FMN and of the FeS clusters induce strong reorganizations of the polypeptide backbone. Additional signals in the spectra of complex I reflect contributions induced by the redox transition of the high-potential FeS cluster N2 which is not present in the NADH dehydrogenase fragment. Part of these signals are attributed to the reorganization of protonated/deprotonated Asp or Glu side chains. On the basis of these data we discuss the role of N2 for proton translocation of complex I.

The NADH:ubiquinone oxidoreductase, also known as respiratory complex I, couples the transfer of electrons from NADH to ubiquinone with the translocation of protons across the membrane. In that way complex I establishes a proton motive force required for energy consuming processes such as synthesis of ATP (*1*, *2*). The bacterial complex I, in general, consists of 14 different subunits, that add up to a molecular mass of approximately 530 kDa (*3*, *4*). Seven subunits are peripheral proteins which contain the binding sites for the known redox groups of complex I, namely one FMN[1] and up to nine iron−sulfur (FeS) clusters. The remaining seven subunits are hydrophobic proteins predicted to fold into 54 α-helices across the membrane. Little is known about their function, but they are most likely involved in ubiquinone reduction and proton translocation (*3*).

The genes of the *Escherichia coli* complex I are organized in the so-called *nuo*-operon (from NADH:ubiquinone oxidoreductase), a 16 kb DNA region localized at min 51 of the chromosome (*5*, *6*). As a special case, the *E. coli* gene *nuo*CD is fused to one gene giving raise to 13 *nuo*-genes, named *nuo*A to *nuo*N (*6*, *7*). The *E. coli* complex I has been isolated in the presence of alkylglycoside detergents by means of chromatographic steps (*8*, *9*). The preparation is solely made up of the 13 different subunits being encoded by the *nuo*-genes. One noncovalently bound FMN, two binuclear (N1b and N1c, nomenclature according to Ohnishi), and three tetranuclear (N2, N3, and N4) EPR detectable FeS clusters are contained in the preparation (*8*, *10*). The FeS clusters N1b, N1c, N3, and N4 are called isopotential clusters because they show similar midpoint potentials in the range from −0.48 to −0.44 V [vs Ag/AgCl (*8*−*10*)]. Together with the FMN ($E_{m,7} = -0.47$ mV), they form the electron input part of complex I involved in NADH oxidation (*8*, *10*). Electrons are transferred from the isopotential FeS clusters to the high-potential cluster N2 ($E_{m,7} = -420$ mV, 8−10), believed to involved in ubiquinone reduction (*8*−*10*).

Upon treatment with salt, the isolated *E. coli* complex I disintegrates into a so-called NADH dehydrogenase fragment, a connecting fragment and a membrane fragment (*6*−*8*). The soluble NADH dehydrogenase fragment comprises the subunits NuoE, F, and G and harbors the FMN and the EPR-detectable FeS clusters N1b, N1c, N3, and N4. The connecting fragment consists of NuoB, CD, and I and contains the EPR-detectable FeS cluster N2. The membrane fragment is composed of the hydrophobic subunits NuoA, H, and J−N and contains a chromophore with a yet unknown chemical structure (*11*−*13*).

† This work is supported by the Deutsche Forschungsgemeinschaft (SFB189/C2 to T.F. and SFB472/P21 to W.M.).

* To whom correspondence should be addressed. E-mail: thorsten.friedrich@uni-duesseldorf.de. Phone: +49-211-8112647. Fax: +49-211-8115310.

‡ Institut für Biophysik.

§ Present address: School of Chemical Sciences, University of Illinois, 600 S. Matthews Street, 61801 Urbana, IL.

|| Institut für Biochemie.

[1] Abbreviations: FAD, flavin adenine dinucleotide; FMN, flavin mononucleotide; SHE′, standard hydrogen electrode (pH 7); vis, visible; FeS, iron sulfur.

10.1021/bi000842a CCC: $19.00
Published on Web 08/11/2000

So far, complex I has been studied mainly by means of EPR- and UV−vis spectroscopy (*14*, *15*) and, in a few cases, also by means of (M)CD- and resonance Raman spectroscopy (*16*, *17*). This led to a spectroscopic characterization of the FMN, the FeS clusters, two forms of semiquinone radicals, and a redox group with a yet unknown chemical structure (*11*−*14*, *18*−*20*). However, the redox-dependent changes in the protein structure and the protonation of the cofactors or individual amino acids have not been studied yet. The combination of FT-IR difference spectroscopy and electrochemistry is a sensitive method to detect redox-dependent changes in protein structure and protonation states of cofactors or amino acid side chains (*21*, *22*). However, this technique has neither been used to characterize complex I nor flavoproteins in general. Here, we report for the first time the electrochemically induced FT-IR difference spectra of the *E. coli* complex I and the NADH dehydrogenase fragment of this complex in H_2O and D_2O buffer. The vibrational modes of the enzyme-bound FMN in both preparations were identified by comparison with electrochemically induced FT-IR difference spectra of free FMN and FAD. Contributions of the individual electron-transfer steps were identified by comparison of the spectra of both preparations for the full and the critical potential steps. Our data indicate that the redox reaction of cluster N2 is coupled to a protonation/deprotonation of an Asp or Glu side chain.

MATERIALS AND METHODS

Sample Preparation. Complex I from *E. coli* and the NADH dehydrogenase fragment of this complex were isolated as previously described (*9*, *23*). For electrochemistry, complex I in 0.15% *n*-dodecyl-*β*-D-maltoside, 50 mM Mes/NaOH, pH 6.0, and 200 mM KCl was concentrated by ultrafiltration (Centricon 100, Amicon) to approximately 0.25 mM. The NADH dehydrogenase fragment in 50 mM Mes/NaOH, pH 6.0, and 200 mM KCl was concentrated by ultrafiltration (Centricon 100, Amicon) to approximately 0.5 mM. FT-IR and vis spectra of FMN (10 mM, Sigma) and FAD (10 mM, Sigma) were recorded in 50 mM Mes/NaOH, pH 6.0, and 200 mM KCl·H_2O was exchanged against D_2O by repeated concentration and dilution of the sample in the D_2O buffer. H/D exchange of amide I protons was found to be better than 70% as judged from the shift of the amide II mode at 1550 cm^{-1} in the FT-IR absorbance spectra (data not shown).

Electrochemistry. The ultrathin layer spectroelectrochemical cell for the UV−vis and IR was used as previously described (*24*). Sufficient transmission in the 1800 to 1000 cm^{-1} range, even in the region of strong water absorbance around 1645 cm^{-1}, was achieved with the cell path length set to 6−8 μm. To avoid complexation of free flavin with the electrode or protein denaturation, the gold grid working electrode was chemically modified by a 2 mM cysteamine solution as reported (*22*). To accelerate the redox reaction, the following mediators were used at a final concentration of 45 μM each (midpoint potential vs Ag/AgCl/3 M KCl in brackets): ferrocenyltrimethylammoniumiodide (+437 mV), 1,1′- dicarboxylferrocene (+436 mV), diethyl-3-methylparaphenylenediamine (+159 mV), ferricyanide (+216 mV), dimethylparaphenylenediamine (+163 mV), 1,1′-dimethylferrocene (+133 mV), tetramethylparaphenylenediamine (+62 mV), tetrachlorobenzoquinone (+72 mV), 2,6-dichlorophenolindophenol (+9 mV), ruthenium hexamine chloride (−8 mV), 1,2-naphthoquinone (−63 mV), trimethylhydroquinone (−108 mV), menadione (−220 mV), 2-hydroxy-1,4-naphthoquinone (−333 mV), anthraquinone-2-sulfonate (−433 mV), neutral red (−515 mV), benzyl viologen (−568 mV), and methyl viologen (−654 mV). At the given concentrations, and with the path length below 10 μm, no spectral contributions from the mediators in the vis and IR range used could be detected in control experiments with samples lacking the protein. Approximately 6−7 μL of the protein solution were sufficient to fill the spectroelectrochemical cell. Potentials quoted with the data refer to the Ag/AgCl/3 M KCl reference electrode; add +208 mV for SHE′ (pH 7) potentials.

Spectroscopy. FT-IR and UV−vis difference spectra as a function of the applied potential were obtained simultaneously from the same sample with a setup combining an IR beam from the interferometer (modified IFS 25, Bruker, Germany) for the 4000 to 1000 cm^{-1} range and a dispersive spectrometer for the 400−900 nm range as reported previously (*21*, *24*). First, the protein was equilibrated with an initial potential at the electrode, and single beam spectra in the vis and IR range were recorded. Then a potential step toward the final potential was applied, and single beam spectra of this state were again recorded after equilibration. Difference spectra were calculated from the two single beam spectra with the initial single beam spectrum taken as reference. No smoothing or deconvolution procedures were applied. The equilibration process for each applied potential was followed by monitoring the electrode current and by successively recording spectra in the visible range until no further changes were observed. The equilibration generally took less than 8 min for the full potential step from −0.7 to 0.2 V. Typically, 128 interferograms at 4 cm^{-1} resolution were coadded for each single beam IR spectrum and Fourier transformed using triangular apodization. 10−15 difference spectra have been averaged.

The FT-IR instrument was purged with dry air to avoid the presence of atmospheric water vapor. Compressed air was predryed in a condensing system, led into a molecular sieve column (Whatman) and was finally passed through a silica gel column. Using this procedure, no water vapor could be detected in control spectra without sample.

RESULTS

Buffer and Model Compounds. The electrochemically induced FT-IR difference spectra contain contributions from the buffer 2-morpholinoethanesulfonic acid (Mes). Figure 1 shows the oxidized-minus-reduced FT-IR difference spectra of Mes/NaOH, pH 6.0, in H_2O (black line) and pD 6.0 in D_2O (gray line) for the potential step from −0.7 to 0.2 V. The protonation/deprotonation of the sulfonate is induced by proton and electron uptake/release from the mediators. The spectra of the Mes buffer in H_2O shows only small difference signals between 1800 and 1300 cm^{-1}, where the major contributions from the protein can be expected. Strong positive modes are present at 1232, 1124, 1084, and 1050 cm^{-1} and negative signals at 1178, 1112, and 1038 cm^{-1}. Upon H/D exchange shifts of 2−5 cm^{-1} are observed and the broad difference band at 1232 cm^{-1} is split to a signal at 1242 and 1206 cm^{-1}. These signals are tentatively assigned

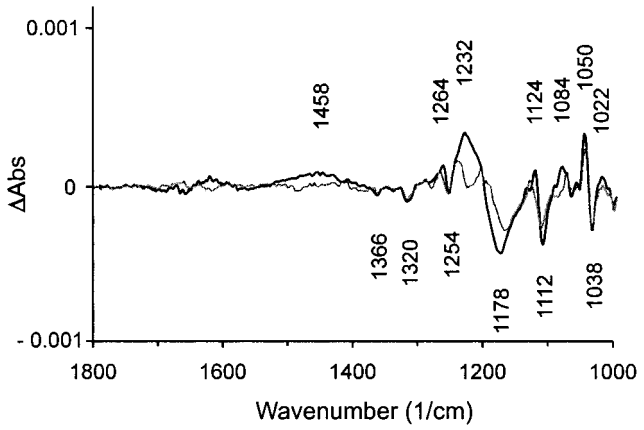

FIGURE 1: Oxidized-minus-reduced FT-IR difference spectra of Mes/NaOH buffer in H_2O (black line) and in D_2O (gray line) for the potential step from −0.7 V to 0.2 V.

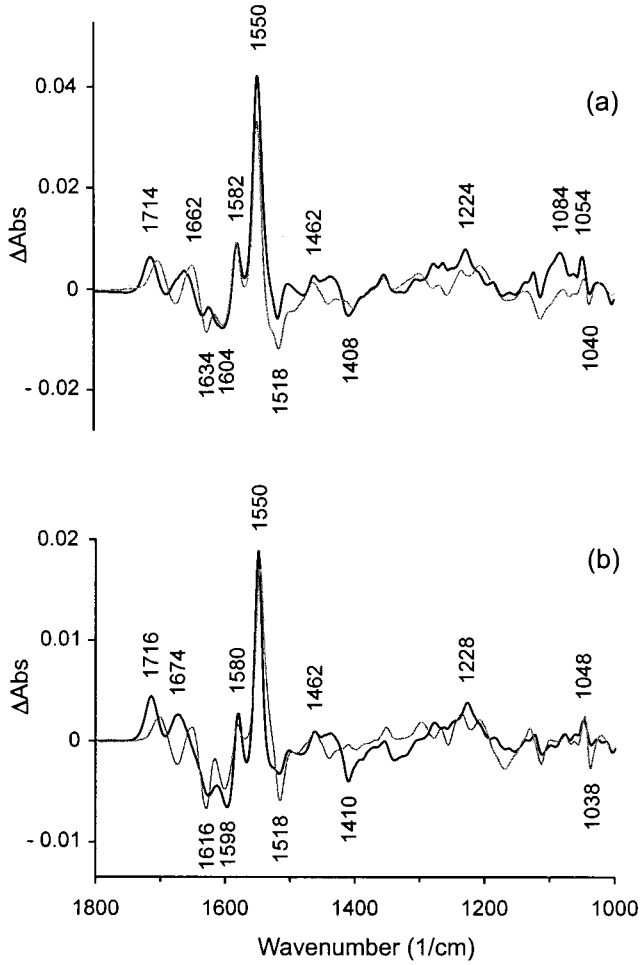

FIGURE 2: Oxidized-minus-reduced FT-IR difference spectra of flavin mononucleotide (a) and of flavin adenin dinucleotide (b) in Mes/NaOH buffer in H_2O (black line) and in D_2O (gray line) for the potential step from −0.5 to 0 V.

to the ν(S═O), δ(OH), ν(C−O), ν(C−N), and ring modes of the 2-morpholinoethanesulfonic acid.

The characteristic contributions of the FMN to the FT-IR spectra of complex I were identified in a model compound study on FMN and FAD. Figure 2 shows the oxidized-minus-reduced FT-IR difference spectra of FMN and FAD in H_2O (black line) and in D_2O (gray line) for the potential step from −0.5 to 0 V in Mes/NaOH, pH 6.0 or pD 6.0. The positive

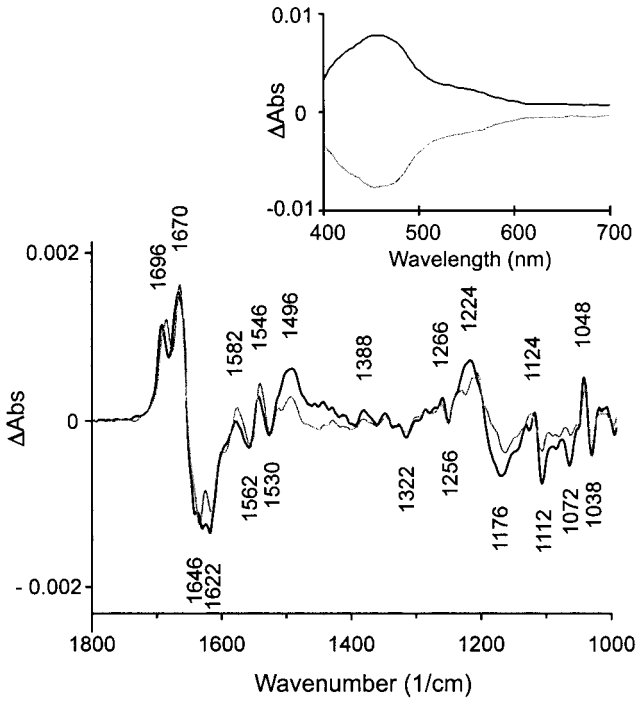

FIGURE 3: Oxidized-minus-reduced FT-IR difference spectra of the NADH dehydrogenase fragment of complex I in Mes/NaOH buffer in H_2O (black line) and in D_2O (gray line) for the potential step from −0.7 to 0.2 V. The inset shows the oxidized-minus-reduced UV−vis difference spectra of the NADH dehydrogenase fragment for the potential step from −0.7 to 0.2 V (black line) and reverse (gray line).

signals correlate with the oxidized flavin and the negative signals with the reduced form.

The spectra are dominated by the strong positive signal of the ν(C═C) mode of neutral flavins at 1550 cm^{-1}. The signals between 1714 and 1634 cm^{-1} are attributed to ν-(C═O) modes, shifting for about 10 cm^{-1} upon H/D exchange caused by the change in hydrogen bonding strength (Figure 2). The signals at 1604 and 1582 cm^{-1} may be assigned to the ν(C═N) modes. Ring modes of the isoalloxazine system contribute in the spectral range between 1460 and 1200 cm^{-1}. These assignments are consistent with resonance Raman data (*25*). The spectra of FAD and FMN are very similar revealing that the reorganizations of the flavin upon electron and proton transfer are essentially limited to the isoalloxazine ring. As a main difference, the P═O mode of the charged phosphate group of FMN can be identified at 1084 cm^{-1} (Figure 2a).

The redox behavior of flavins is highly complex (*26*). Monomeric and dimeric species are involved in the equilibrium reactions of the oxidized and reduced forms from FMN, $FMNH_2$, and free radical $FMNH^{\cdot}$. Therefore, the infrared spectra could include contributions of semiquinoid and dimeric species (*27*). Spectral contributions of various flavin adducts are reflected in the variation of the amplitude of the difference signals at 1515 and 1530 cm^{-1} and between 1714 and 1408 cm^{-1} at high flavin concentrations. However, the vis spectra clearly showed that the contributions of flavin adducts to the spectra are less than 10% at the chosen concentrations (data not shown). This is in agreement with the reported data (*27*).

NADH Dehydrogenase Fragment. The inset in Figure 3 presents the oxidized-minus-reduced vis difference spectra

of the NADH dehydrogenase fragment of complex I for the potential step from −0.7 to 0.2 V (black line) and reverse (gray line). The difference spectra are mirror images indicating the full reversibility of the electrochemical reaction. The broad and unpronounced difference signal shows a maximum at approximately 460 nm and is attributed to overlapping contributions from the FMN as well as from the FeS clusters. The major absorptions stem from the FMN at 370 and 456 nm with a shoulder at 472 nm (*28*). Small contributions of the binuclear clusters N1b and N1c are present at 460 and 550 nm (*29*) and of the tetranuclear clusters N3 and N4 at approximately 415 nm (*30*).

Figure 3 shows the oxidized-minus-reduced FT-IR difference spectra of the NADH dehydrogenase fragment in H_2O (black line) and in D_2O (gray line) for the potential step from −0.7 to 0.2 V. In the electrochemically induced FT-IR difference spectra contributions can be expected from reorganizations of secondary structure elements, from the FMN and from individual amino acids concomitant with electron transfer and proton translocation. While the FeS modes do not contribute in the studied spectral range (*31*) contributions of the ligands can be expected.

The ν(C═O) modes of protonated aspartic and glutamic acid side chains contribute in the spectral range between 1800 and 1710 cm^{-1}. Beside a very small shoulder at about 1710 to 1720 cm^{-1}, no significant difference signal can be observed in difference spectra from the NADH dehydrogenase fragment for the full potential step (Figure 3). In the amide I range from 1700 to 1620 cm^{-1} modes at 1696, 1670, 1646, 1634, and 1622 cm^{-1} can be seen. This spectral range is characteristic for β-sheet secondary structure elements and loops (*32*). In addition to secondary structure elements, contributions from C═O modes of the FMN and of individual amino acid side chains, in particular Asn, Gln, or Arg, are conceivable in this spectral range (*33*). In the amide II range from 1570 to 1520 cm^{-1} signals from the coupled C═N stretching and N−H bending modes are expected to contribute. However, this assignment is improbable since no shift of these signals upon H/D exchange is observed (Figure 3, gray line). Contributions of ringmodes of the FMN isoalloxazine ring and from antisymmetric COO^- modes of deprotonated Asp or Glu side chains are also expected in that range. In the lower spectral range from 1300 to 1000 cm^{-1} contributions from the buffer reflecting the proton uptake of the FMN can be seen (cf. Figure 2).

To distinguish the modes coupled to the FMN in the NADH dehydrogenase fragment, critical potential steps concomitant with the midpoint potential of FMN were studied and compared with the spectra of FMN (Figure 2). The midpoint potential of FMN in complex I as well as in the NADH dehydrogenase fragment at pH 6.0 is −0.53 V vs Ag/AgCl according to an electrochemical titration (P. Hellwig, S. Bungert, and T. Friedrich, unpublished results). The electrochemically induced FT-IR difference spectra of the NADH dehydrogenase fragment for the potential step from −0.7 to −0.5 V, thus, contains the main contributions from the FMN (Figure 4a). On the basis of the model compound spectra (Figure 2b) the ν(C═C) mode can be identified at 1548 cm^{-1}, absorbing at a position close to free flavin in solution. The ν(C═O) mode can be seen at 1710 cm^{-1}, close to the position observed in aqueous solution and thus indicating the presence of hydrogen bonding of the protein to the C═O group.

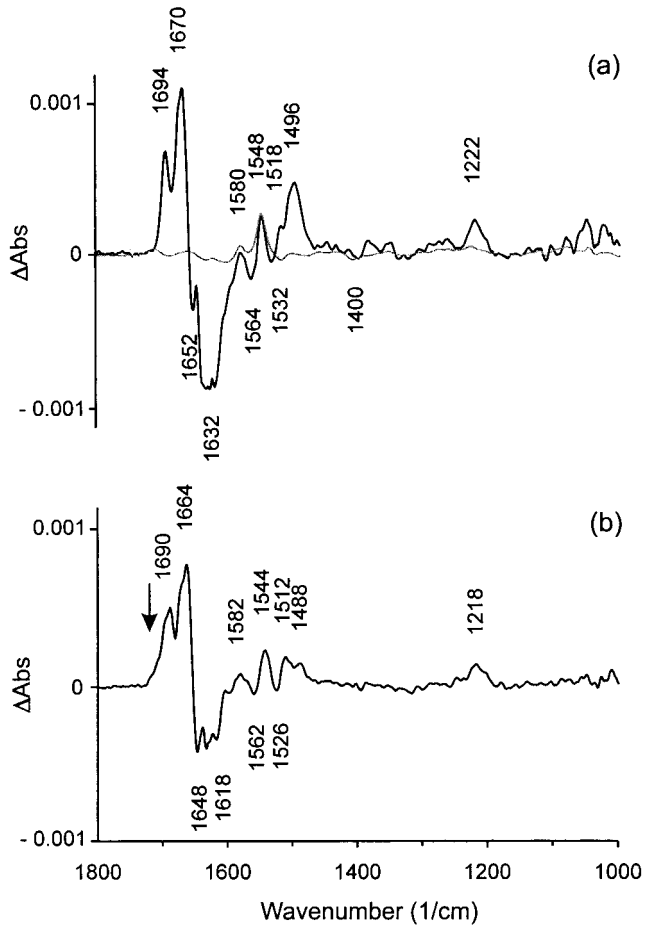

FIGURE 4: Oxidized-minus-reduced FT-IR difference spectra of the NADH dehydrogenase fragment of complex I for the critical potential steps from −0.7 to −0.5 V (a) and from −0.5 to −0.3 V (b). The gray line in panel a represents the oxidized-minus-reduced difference spectra of pure FMN as obtained in Figure 2 calculated to the same concentration as the NADH dehydrogenase fragment. The shoulder at about 1710 to 1720 cm^{-1} is marked with an arrow.

Differences in the hydrogen bonding of the protein bound and free flavin is reflected by shifts of, i.e., the C═O modes or the C═N modes, superimposed by the significantly stronger amide I modes at 1696 cm^{-1}. The expected shift upon H/D exchange (cf Figure 2) may be overlapped by other signals. Further FMN modes are involved in signals at 1580, 1222, 1632, 1694, and 1672 cm^{-1}. The signal at 1084 cm^{-1} in Figure 2a discussed to stem from the charged phosphate group of FMN is not present in the electrochemically induced FT-IR difference spectra of the NADH dehydrogenase fragment (Figure 3), showing that this group does not rearrange or change its protonation state upon the redox reaction within the protein. In conclusion, the spectral contributions of the FMN to the electrochemically induced FT-IR difference spectra of the NADH dehydrogenase fragment of complex I are unexpectedly small.

The amide I region from 1690 to 1630 cm^{-1} of the spectra for the potential step from −0.7 to −0.5 V (Figure 4a) is dominated by strong positive signals at 1694 and 1670 cm^{-1} and strong negative modes at 1652 and 1632 cm^{-1} reflecting a large reorganization of the polypeptide backbone. Modes at 1564, 1548, 1532, 1518, and 1496 cm^{-1} contribute in the

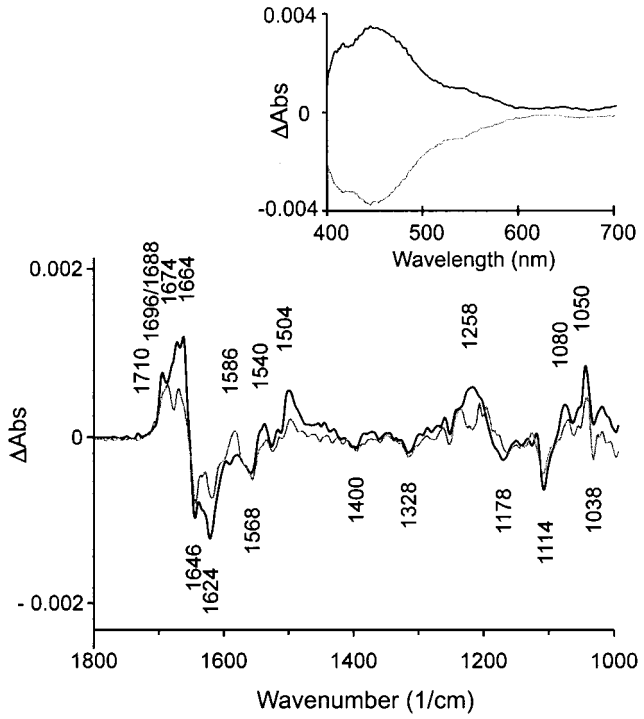

FIGURE 5: Oxidized-minus-reduced FT-IR difference spectra of complex I in Mes/NaOH buffer in H_2O (black line) and in D_2O (gray line) for the potential step from −0.7 to 0.2 V. The inset shows the oxidized-minus-reduced UV−vis difference spectra of complex I for the potential step from −0.7 to 0.2 V (black line) and reverse (gray line).

amide II region. Since only a small shift at these positions is observed upon H/D exchange (Figure 3), an attribution to amide II modes is not very conceivable, except for not exchangeable amide protons. It is more likely although tentative that these absorptions stem from individual amino acids such as tyrosines and deprotonated Asp and Glu side chains.

The FeS clusters N1b, N1c, N3, and N4 of the NADH dehydrogenase fragment show a pH-independent midpoint potential from −0.48 to −0.44 V (*8*). The electrochemically induced FT-IR difference spectra for the potential step from −0.5 to −0.3 V therefore reflects reorganizations of the enzyme upon electron transfer via the FeS clusters (Figure 4b). It is noteworthy to mention that this spectra shows a very small shoulder at about 1710 to 1720 cm^{-1}. In this range, the ν(C═O) mode from protonated Asp and Glu side chains are expected. This signal may thus be caused by protonation of such a side chain or by pertubation of a protonated group upon a change of a local environment due to the electron transfer via the FeS clusters.

NADH:Ubiquinone Oxidoreductase. The inset in Figure 5 shows the oxidized-minus-reduced vis difference spectra of complex I for the potential step from −0.7 to 0.2 V (black line) and reverse (gray line). The broad difference signal comprises the strongly overlapping contributions from the FMN and the FeS clusters as described for the NADH dehydrogenase fragment above. The broad absorption around 415 nm is larger than in the NADH dehydrogenase fragment due to the presence of the additional tetranuclear FeS cluster N2, and to a yet unclassified chromophore in the membrane fragment of the complex (*11*−*13*).

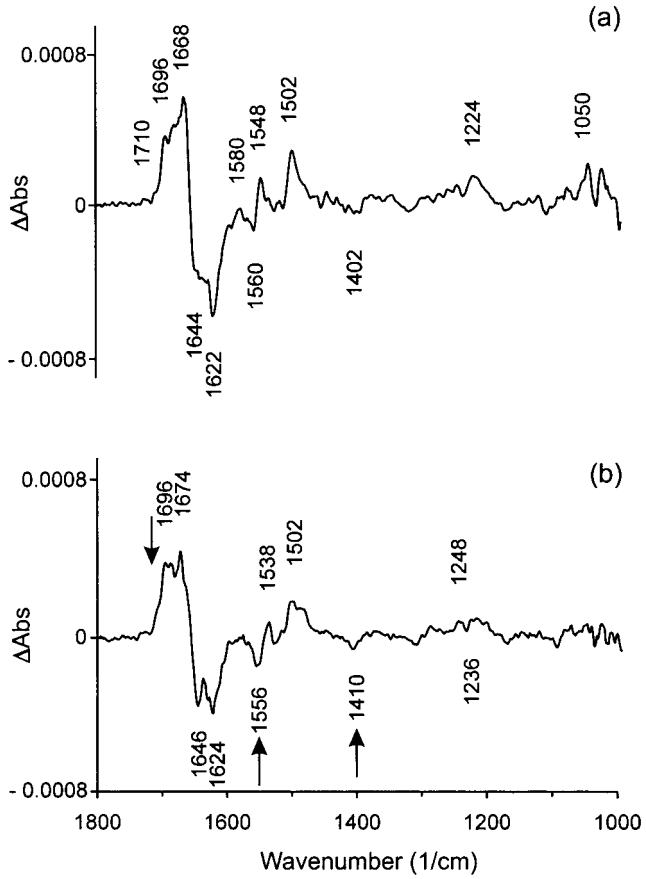

FIGURE 6: Oxidized-minus-reduced FT-IR difference spectra of complex I for the critical potential steps from −0.7 to −0.5 V (a) and from −0.5 to −0.3 V (b). The signals at about 1710 to 1720, 1556, and 1410 cm^{-1} discussed to stem from the protonation of an Asp or Glu side chain are marked with arrows.

Figure 5 shows the oxidized-minus-reduced FT-IR difference spectra of complex I in H_2O (black line) and in D_2O (gray line) for the potential step from −0.7 to 0.2 V. Clear differences are present with respect to the corresponding spectra of the NADH dehydrogenase fragment (Figure 3). To work out these differences, spectra of the critical potential steps have been studied.

Figure 6a shows the spectra obtained for the critical potential step from −0.7 to −0.5 V with the contribution of the FMN as a small positive signal at 1548 cm^{-1} as identified by comparison with the spectra of FMN (Figure 2a). The shoulder at 1710 cm^{-1} may be attributed to the ν(C═O) mode of the FMN. However, as already observed in the spectra of the NADH dehydrogenase fragment (Figure 3), a characteristic downshift of the mode for about 6 cm^{-1} upon H/D exchange like in FMN (Figure 2a) cannot be seen. This may be attributed to a spectral overlap with other signals, which is conceivable on the basis of the intensity of the signal expected (Figure 2a). The signal at 1710 cm^{-1} does not only derive from the enzyme bound FMN, but contains additional contribution(s) from other group(s) since it has a higher intensity in comparison with the signal at 1548 cm^{-1} of free FMN (Figure 2a). As in the NADH dehydrogenase fragment, the FMN contributes only a few and weak bands to the electrochemically induced FT-IR difference spectra of complex I.

Figure 6b shows the spectra obtained from the critical potential step from −0.5 to −0.3 V. The additional signals

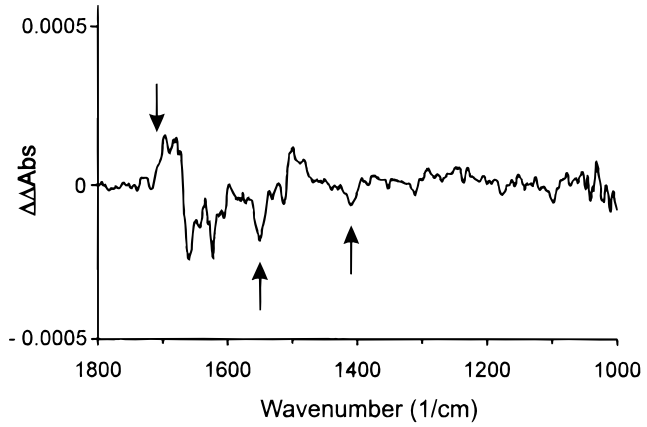

FIGURE 7: Double difference FT-IR spectrum of oxidized-minus-reduced difference spectra of complex I (Figure 6b) minus oxidized-minus-reduced difference spectra of NADH dehydrogenase fragment (Figure 4b) for the critical potential step from −0.5 to −0.3 V. The signals at about 1716 to 1712, 1555 to 1580, and 1402 to 1404 cm^{-1} discussed to stem from the protonation of an Asp or Glu side chain are marked with arrows.

that are present in these spectra as compared to the spectra of the NADH dehydrogenase fragment (Figure 4b) are proposed to derive from reorganizations of the protein environment upon electron transfer and concomitant proton transfer to cluster N2 with a midpoint potential of −0.37 V at pH 6.0 (8). The FeS cluster N2 is not present in the NADH dehydrogenase fragment. Additional signals are present in the amide I range at 1696, 1674, and 1624 cm^{-1}. New signals also arise in the amide II range at 1556, 1538, and 1502 cm^{-1}. In the spectral range characteristic for protonated Asp and Glu side chains, the intensity of the shoulder at about 1710 to 1720 cm^{-1} is significantly increased as compared to the spectra of the NADH dehydrogenase fragment in the same potential range (Figure 4b). This signal is tentatively attributed to a ν(C═O) mode of either an Asp or Glu side chain which is protonated in the oxidized form or to a pertubation of a protonated group upon a change of a local environment. Since this signal is much more intense as in the spectra of the NADH dehydrogenase fragment, we assume that it is coupled to the electron-transfer involving cluster N2. The signals observed at 1556 and 1410 cm^{-1} are tentatively interpreted as $\nu(COO^-)^{s/as}$ modes. These signals are expected, if the shoulder at 1710−1720 cm^{-1} would indeed derive from a deprotonation of an Asp or Glu side chain upon reduction of N2.

The spectral contributions due to the redox reaction of N2 are shown in the double difference spectrum of the spectra of complex I (Figure 6b) minus the spectra of NADH dehydrogenase fragment (Figure 4b) for the critical potential step from −0.5 to −0.3 V (Figure 7). Besides rearrangements of the polypeptide backbone upon electron transfer to and from N2, contributions of individual amino acids such as asparagine, tyrosine, glutamine, or arginine side chains could be present in the spectra, compared to the spectral positions of single amino acids in solution (*33*). These assignments are highly tentative and need to be confirmed by site directed mutagenesis in combination with FT-IR spectroscopy. However, the signals we attribute to the protonation of aspartic or glutamic acid side chain(s) are clearly visible. The ν(C═O) mode of protonated aspartic or glutamic acids contributes at 1716−1712 cm^{-1} in aqueous solutions. The respective signals for the deprotonated forms are observed at 1555−1580 cm^{-1} [$\nu(COO^-)^{as}$] and at 1402−1404 cm-1 [$\nu(COO^-)^{s}$] (*33*). The relative intensity of these signals fits very well with the one reported (*33*). This might indicate that the observed residue(s) probably exposed to an aqueous environment.

DISCUSSION

The progress in complex I research is hampered by its enormous complexity. While a picture of the electron pathway is beginning to emerge (*12*, *14*) the molecular mechanism of its coupling to proton translocation is not understood, although several proposals have been made (*34*, *35*). To determine the electron transfer step(s) in complex I which might be involved in proton translocation, we set out to advance FT-IR spectroscopy of electrochemically adjusted redox states of complex I.

The combination of FT-IR difference spectroscopy and electrochemistry has been successfully applied to describe various proteins (*22*, *24*, *36*−*39*). This method had to be adapted to investigate complex I. First, both preparations had to be highly concentrated without aggregation to maintain reactivity and to avoid light scattering. The preparation of the soluble NADH dehydrogenase fragment (*23*) was concentrated to higher than 0.5 mM without changing its catalytic activity and its spectroscopic properties. Using the same criteria, the preparation of complex I in dodecyl maltoside (*9*) could be concentrated up to 0.3 mM. Since the equilibration times were longer than 30 min at this concentration, we used a 0.25 mM complex I aliquot for the measurements. Second, it was not clear whether the combination of electrochemistry and FT-IR spectroscopy can be appplied to such a huge protein with a molecular mass of 535 kDa. Using the chemically modified gold grid electrode and the mediators as described in Material and Methods, we obtained reduced-minus-oxidized difference spectra which were identical to the ones obtained by chemical reduction with dithionite or NADH (*7*, *9*). The electrochemically induced reduction and oxidation of complex I as well as of the NADH dehydrogenase fragment was completely reversible (Figures 3 and 5). Under this conditions we acquired for the first time FT-IR spectra of complex I and the NADH dehydrogenase fragment of this complex.

Comparison of FT-IR spectra of free FMN and FAD with the spectra of both preparations led to the attribution of vibrational modes of the enzyme-bound flavin. The positive signals at 1710 and 1548 cm^{-1} of the ν(C═O) modes of the isoalloxazine ring are the only detectable contributions of FMN in complex I as well as in the NADH dehydrogenase fragment (Figures 2, 3, and 5). Spectra for the critical potential step revealed that these contributions are small (Figures 4a and 5a).

The spectra of complex I and the NADH dehydrogenase fragment are dominated by large rearrangements of the protein during electron transfer. This is in accordance with cross-link and labeling studies with oxidized and reduced complex I. Different reactivities are obtained from complex I in different redox states (*40*−*42*). This indicates that the redox reaction of complex I is accompanied by major structural changes. It is not clear, however, whether these conformational changes are related to proton pumping in complex I.

The electron transfer from the FMN to the isopotential FeS clusters results mainly in local protein rearrangements. A small shoulder at about 1710−1720 cm^{-1} is seen in the spectra for the critical potential step of the NADH dehydrogenase fragment (Figure 4b). The corresponding spectra of complex I (Figure 6b) contains additional signals arising from the electron transfer from the isopotential FeS clusters to cluster N2. The shoulder around 1710 to 1720 cm^{-1} is much more intense in the spectra of complex I compared to the signal in the spectra of the NADH dehydrogenase fragment (Figures 4b and 6b). This implies that either the oxidation of N2 is most likely coupled with the protonation of an Asp or Glu side chain or that such a side chain is protonated in both, the oxidized and reduced state of N2 and experiences a change in its local environment upon electron transfer to N2. In the latter case the observed modes at 1556 and 1410 cm^{-1} would arise from the redox transition of a different group. Both processes would change the extinction coefficient leading to the mode around 1710−1720 cm^{-1} and studies involving site-directed mutants are required to discriminate both possibilities.

The midpoint potential of N2 is pH dependent, which has led to the assumption that N2 is involved in proton translocation (*43*). Its role as a redox Bohr group has been discussed (*34*). The pH dependence of N2 exhibits a slope of −60 mV/pH (*43*) implying that the reduced state of N2 receives a proton and the oxidized state of N2 becomes deprotonated. However, our data indicate that an Asp or Glu side chain is protonated coupled to the oxidation of N2. Thus, the protonation observed cannot represent the protonation of a redox Bohr group associated with N2. As a working hypothesis, we speculate that the proton being released from N2 upon oxidation is picked up by an acidic amino acid. The involvement of such an group in the proton pumping activity of complex I is conceivable. We were not able to detect a signal which might be attributed to the deprotonation of an Asp or Glu side chain as expected for a redox Bohr group associated with N2 at any potential step.

It has been shown that complex I and a family of membraneous multisubunit hydrogenases share a common anchestor (*44*). Among these hydrogenases the so-called Ech hydrogenase of the methanogenic archaeon *Methanosarcina barkeri* has been biochemically characterized (*45*, *46*). The Ech-hydrogenase is composed of six subunits four of them being homologous to subunits of the connecting fragment of the *E. coli* complex I while the remaining two are homologous to hydrophobic subunits of the membrane fragment. This hydrogenase most likely works as a proton pump (*45*−*47*). It is an attractive hypothesis that the protonation of an acidic amino acid associated with the oxidation of N2 described in this work is the molecular switch involved in proton translocation in complex I as well as in the Ech hydrogenase. This module common to complex I and the membraneous multisubunit hydrogenases may represent a conserved device for the translocation of one proton per electron.

ACKNOWLEDGMENT

We are grateful to Christine Ernd and Monika Kerstan for excellent technical assistance.

REFERENCES

1. Weiss, H., Friedrich, T., Hofhaus, G., and Preis, D. (1991) *Eur. J. Biochem. 197*, 563−576.
2. Walker, J. E. (1992) *Q. Rev. Biophys. 25*, 253−324.
3. Friedrich, T., Steinmüller, K., and Weiss, H. (1995) *FEBS Lett. 367*, 107−111.
4. Yagi, T., Yano, T., DiBernardo, S., and Matsuno-Yagi, A. (1998) *Biochim. Biophys. Acta 1364*, 125−133.
5. Weidner, U., Geier, S., Ptock, A., Friedrich, T., Leif, H., and Weiss, H. (1993) *J. Mol. Biol. 233*, 109−122.
6. Friedrich, T. (1998) *Biochim. Biophys. Acta 1364*, 134−146.
7. Braun, M., Bungert, S., and Friedrich, T. (1998) *Biochemistry 37*, 1861−1867.
8. Leif, H., Sled', V. D., Ohnishi, T., Weiss, H., and Friedrich, T. (1995) *Eur. J. Biochem. 230*, 538−548.
9. Spehr, V., Schlitt, A., Scheide, D., Guénebaut, V., and Friedrich, T. (1999) *Biochemistry 38*, 16216−16267.
10. Sled′, V. D., Friedrich, T., Leif, H., Weiss, H., Meinhardt, S. W., Fukumori, Y., Calhoun, M. W., Gennis, R. B., and Ohnishi, T. (1993) *J. Bioenerget. Biomembr. 25*, 347−357.
11. Schulte, U., Abelmann, A., Amling, N., Brors, B., Friedrich, T., Kintscher, L., Rasmussen, T., and Weiss, H. (1998) *BioFactors 8*, 177−186.
12. Schulte, U., Haupt, V., Abelmann, A., Fecke, W., Brors, B., Rasmussen, T., Friedrich, T., and Weiss, H. (1999) *J. Mol. Biol. 292*, 569−580.
13. Friedrich, T., Abelmann, A., Brors, B., Guenebaut, V., Kintscher, L., Leonard, K., Rasmussen, T., Scheide, D., Schlitt, A., Schulte, U., and Weiss, H. (1998) *Biochim. Biophys. Acta 1365*, 215−219.
14. Ohnishi, T. (1998) *Biochim. Biophys. Acta 1364*, 186−207.
15. Hatefi, Y. (1985) *Annu. Rev. Biochem. 54*, 1015−1069.
16. Kowal, A. T., Morningstar, J. E., Johnson, M. K., Ramsay, R. R., and Singer, T. P. (1986) *J. Biol. Chem. 261*, 9239−9245.
17. Crouse, B. R., Yano, T., Finnegan, M. G., Yagi, T., and Johnson, M. K. (1994) *J. Biol. Chem. 269*, 21030−21036.
18. Sled', V. D., Rudnitzky, N. I., Hatefi, Y., and Ohnishi, T. (1994) *Biochemistry 33*, 10069−10075.
19. Vinogradov, A. D., Sled', V. D., Burbaev, D. S., Grivennilova, V. G., Moroz, I. A., and Ohnishi, T. (1995) *FEBS Lett. 370*, 83−87.
20. van Belzen, R., Kotlyar, A. B., Moon, N., Dunham, W. R., and Albracht, S. P. J. (1997) *Biochemistry 36*, 886−893.
21. Mäntele, W. (1993) *Trends Biochem. Sci. 18*, 197−202
22. Hellwig, P., Behr, J., Ostermeier, C., Richter, O.-M. H., Pfitzner, U., Odenwald, A., Ludwig, B., Michel, H., and Mäntele, W. (1998) *Biochemistry 37*, 7390−7399.
23. Bungert, S., Krafft, B., Schlesinger, R., and Friedrich, T. (1999) *FEBS Lett. 460*, 207−211.
24. Moss, D. A., Nabedryk, E., Breton, J., and Mäntele, W. (1990) *Eur. J. Biochem. 187*, 565−572.
25. Visser, A. J., Vervoort, J., O'Kane D. J., Lee, J., and Carreira, L. A. (1983) *Eur. J. Biochem. 131*, 639−645.
26. Swinheart, J. H. (1966) *J. Am. Chem. Soc. 88*,1056−1058.
27. Beinert, H. (1956) *J. Am. Chem. Soc. 78*, 5323−5328.
28. Gishla, S. (1980) *Methods Enzymol. 66*, 360−373.
29. Dailey, H. A., Finnegan, M. G., and Johnson, M. K. (1993) *Biochemistry 33*, 403−407.
30. Malkin, R. (1973) in *Iron−sulfur Proteins* (Lovenberg, W., Ed.) Vol. 2, pp 235−244; Academic Press, Orlando, FL.
31. Herzberg, G. (1962) in *Molecular spectra and molecular structure: II. Infrared and Raman spectra of polyatomic molecules*, D. Van Nostrand Company, Inc. Pricenton, NJ.
32. Arrondo, J. L. R., Muga, A., Castresana, J., and Goni, F. M. (1993) *Prog. Biophys. Mol. Biol. 59*, 23−56.
33. Venyaminov, S. Y., and Kalnin, N. N. (1990) *Biopolymers 30*, 1259−1271.
34. Brandt, U. (1997) *Biochim. Biophys. Acta 1318*, 79−91.
35. Dutton, P. L., Moser, C. C., Sled, V. D., Daldal, F., and Ohnishi, T. (1998) *Biochim. Biophys. Acta 1364*, 245−257.
36. Baymann, F., Roberson, D. E., Dutton, P. L., and Mäntele, W. (1999) *Biochemistry 38*, 13188−13199.

37. Hellwig, P., Soulimane, T., Buse, G., and Mäntele, W. (1999) *FEBS Lett. 458*, 83−86.
38. Hellwig, P., Mogi, T., Tomson, F. L., Gennis, R. B., Iwata, J., Miyoshi, H., and Mäntele, W. (1999) *Biochemistry 38*, 14683−14689.
39. Hellwig, P., Soulimane, T., Buse, G., and Mäntele, W. (1999)- *Biochemistry 38*, 9648−9658.
40. Gondal, J. A., and Anderson, W. M. (1985) *J. Biol. Chem. 260*, 12690−12694.
41. Belogrudov, G. I., and Hatefi, Y. (1994) *Biochemistry 33*, 4571−4576.
42. Yamaguchi, M., Belogrudov, G. I., and Hatefi, Y. (1998) *J. Biol. Chem. 273*, 8094−8098.
43. Ingledew, W. J., and Ohnishi, T. (1980) *Biochem. J. 186*, 111−117.
44. Friedrich, T., and Weiss, H. (1997) *J. Theor. Biol. 187*, 529−540.
45. Künkel, A., Vorholt, J. A., Thauer, R. K., and Hedderich, R. (1998) *Eur. J. Biochem. 252*, 467−476.
46. Meuer, J., Bartoschek, S., Koch, J., Künkel, A., and Hedderich, R. (1999) *Eur J. Biochem. 265*, 325−335.
47. Bott, M., and Thauer, R. K.(1989) *Eur. J. Biochem. 179*, 469−472.

BI000842A